CSM
Chemistry of Solid Materials
Vol. 2 No. 2, 2014-2015

Facile Synthesis and Spectroscopic Studies of SiO_2-Core/ZnS-Shell Nanostructure

M. Kazemipour[1], A. Pourahmad*[2]

[1]MSc Student, Department of Chemistry, Rasht Branch, Islamic Azad University, Rasht, Iran
[2]Associate Professor, Department of Chemistry, Rasht Branch, Islamic Azad University, Rasht, Iran
** Corresponding author's E-mail: Pourahmad@iaurasht.ac.ir*

ABSTRACT
SiO_2/ZnS core/shell nanostructures have been synthesized at room temperature by a simple wet chemical method. The prepared materials are characterized by X-ray diffraction (XRD), scanning electron microscopy (SEM), infrared spectroscopy (IR), UV–vis spectroscopic and transmission electron microscopy (TEM) studies. X-ray diffraction pattern exhibits peaks correspond to the cubic phase of ZnS. The morphological studies revealed the uniformity in size distribution with core size of 250 nm and shell thickness of 14 nm. From UV–Vis spectra the band gap energies are calculated. The band gap of ZnS has been determined as 3.70 eV directly from the absorption maximum of ZnS, λ_{max} = 335 nm. The band gap of the bulk ZnS is 3.54 eV.

Keywords: Nanostructured materials, Chemical synthesis, Optical properties, Transmission electron microscopy (TEM), X-ray diffraction

1. INTRODUCTION

Semiconducting nanomaterials are of great interest for their unique size dependent optical and electrical properties. Fabrication and morphology control of materials is a crucial issue in material research. The materials with highly controlled structures and uniform morphologies may lead to novel physical and chemical properties in contract with the non-controlled, which make them enormous potential for a wide spectrum of application [1–3]. ZnS is non-toxic, abundant and cheap. Zinc sulphide (ZnS), an important semiconductor compound of the IIB-VI groups, is mostly found in one of two structural forms cubic sphalerite or hexagonal wurtzite, which have wide band gaps of 3.54 eV and 3.80 eV at 300 K, respectively. The wider band gap of ZnS enables high energy incident photons to reach the window-absorber junction, enhancing the blue response of the photovoltaic cells and thus contributes to a better cell per-formance. ZnS nanocrystals are also good photocatalysts because of the rapid generation of electron–hole pairs by photo-excitation and the highly negative reduction potentials of excited electrons, and it has been intensively

studied because of its unique catalytic functions compared to those of TiO_2 [4]. Zinc sulphide (ZnS), as a very important semiconductor material, has been widely used in emission, fuel cells, solar energy conversion, photocatalysis, light emitting diode and so on [5–8]. However, ZnS nanoparticles are easy to aggregate, which greatly limits its excellent photoelectric properties. The ways to solve the problems of ZnS include combining ZnS with noble metals, or loading ZnS on support materials which have high surface areas and conductivity [9]. In this article, we report our recent investigations on structural, morphological and optical properties of SiO_2/ZnS core/shell nanomaterials. At first we synthesize silica particles then ZnS nanoparticles are deposited on SiO_2 as a shell material by using the simple wet chemical method to form SiO_2-core/ ZnS-shell nanostructures.

2. EXPERIMENTAL

2.1. Preparation of SiO_2-core/ZnS-shell nanoparticles

All the chemical reagents were commercial with analytical grade purity, and used directly without further purifications. We followed the Stobber process of silica particle synthesis. In a typical synthesis, cetyltrimethylammonium bromide (CTAB) of 0.5 g, ammonia solution of 30 ml and ethanol of 80 ml were mixed in 100 ml of water. Then 600 µl of tetra ethyl orthosilicate have been added. After 1 h the white powders were collected by centrifugation and dispersed in Zinc acetate (0.3 g in 100 ml) solution. After 5 min, the powders were collected back by centrifugation and then washed with water. Then dispersed again in the sodium sulphide solution (0.3 g in 100 ml) and then collected back for drying. The dried powder was directly taken into further characterizations.

2.2. Characterization

Powder X-ray diffraction patterns of the samples were recorded using an X-ray diffractometer (Bruker D8 Advance) with Co Kα radiation (λ= 1.789 Å) under the conditions of 40 kV and 30 mA, at a step size of 2θ = 0.02°. The UV–Vis diffused reflectance spectra (UV–Vis DRS) obtained from UV–Vis Scinco 4100 spectrometer with an integrating sphere reflectance accessory. $BaSO_4$ was used as reference. The infrared spectra on KBr pellet were measured on a Bruek spectrophotometer. The transmission electron micrographys (TEM) were recorded with a Philips CM10 microscope, working at a 100 kV accelerating voltage. Samples for TEM were prepared by dispersing the powdered sample in acetone by sonication and then drip drying on a copper grid coated with carbon film. The surface morphology of the samples was obtained using a Jeol-JSM-5610 LV scanning electron microscopy (SEM).

3. RESULTS AND DISCUSSION

The liquid crystal templating has been used here for the formation of SiO_2 spheres, then SILAR assisted ZnS shell layer is formed over the SiO_2 spheres. At first, the CTAB micelles are formed above the critical micelle concentration. Then silicate ions are precipitating over the head groups of CTAB due to complementary of charges. After this, hydrolysis followed by condensation of silicates allows to form silica formations [10]. Due to the negative surface charges of silica in water at pH 5.8, dispersion of silica spheres tolerates the Zn^{2+} ions to get adsorb over it. Finally the immersing of formed Silica/Zn^{2+} in the solution of S^{2-} will form the SiO_2-core/ZnS-shell

nanostructures. The crystallinity of the Silica spheres, SiO_2/ZnS core–shell nanoparticles were studied by XRD. The sharp amorphous peak at 22° indicates the uniformity of silica spheres (Fig. 1) as reported elsewhere [11]. The XRD pattern of synthesized powder for Silica/ZnS nanoparticles are shown in Fig. 2. It shows several diffraction peaks at 2θ values of 28.1, 48.3 and 59.2, which correspond to the Miller index of the reflecting planes for (111), (220) and (222). The XRD peaks of ZnS nanocrystals, indicate a sphalerite-type cubic structure and space group (F-43 m) in good agreement with the JCPDS card 05-0566, confirming the formation of ZnS nanparticles. The amorphous peak of silica at 22° is not identified in the pattern of the SiO_2/ZnS. This may be due to complete coverage of silica by the shell layer. No other impurity peaks in the diffraction pattern indicate the purity of SiO_2/ZnS core–shell system. Further the widened full width at half maximum (FWHM) of peaks in the ZnS diffraction pattern indicates the smaller layer thickness [12].

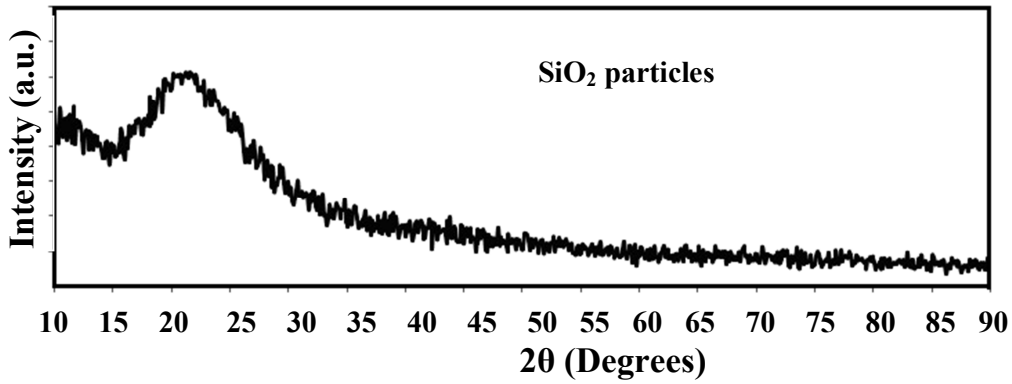

Fig. 1. XRD pattern of SiO_2.

SEM images of SiO_2 particles and SiO_2/ZnS nanostructures are shown in Fig. 3(a-d). Fig. 3a and b shows SEM images of SiO_2 particles. A panoramic SEM image in Fig. 3a demonstrates that the obtained pure SiO_2 powder shows spherical morphology on a large scale. These spheres are relatively unique in size, with a diameter ~250 nm. Moreover, high magnification SEM images in Fig. 3b show that the surface of the composite is basically smooth. Fig. 3c–d shows the images of the Silica/ZnS nanostructures. It can be seen that the sphere surfaces were not as smooth as that of pure SiO_2, due to the formation of nanosized ZnS particles. The sizes of the SiO_2/ZnS nanostructures are about 300 nm.

The FT-IR spectrums of these nanostructures are shown in Fig. 4. FT-IR spectrum of silica shows the characteristic vibrations of SiO_2 and CTAB (Fig. 4a). The vibrations at 1057, 791 and 454 cm^{-1} are the respective to Si–O–Si, Si–O, O–Si–O bonds. Vibrations occurred at 962 and 1645 cm^{-1} are for stretching of non bridging oxygen atoms present in unreacted Si–OH group and weak bending vibration of H–O–H in H_2O. The CTAB can be realized at the wave numbers 2853, 2922 cm^{-1} (tail group vibrations), 1477 cm^{-1} (head group vibration). The spectrum taken for Silica/ZnS (Fig. 4b) remarked a few noteworthy changes in the observed vibrations of silica particles. The characteristic vibrations of CTAB and SiO_2 decrease in its intensity, after the ZnS layer formed over the silica. The intensity of N–CH bonding stretching

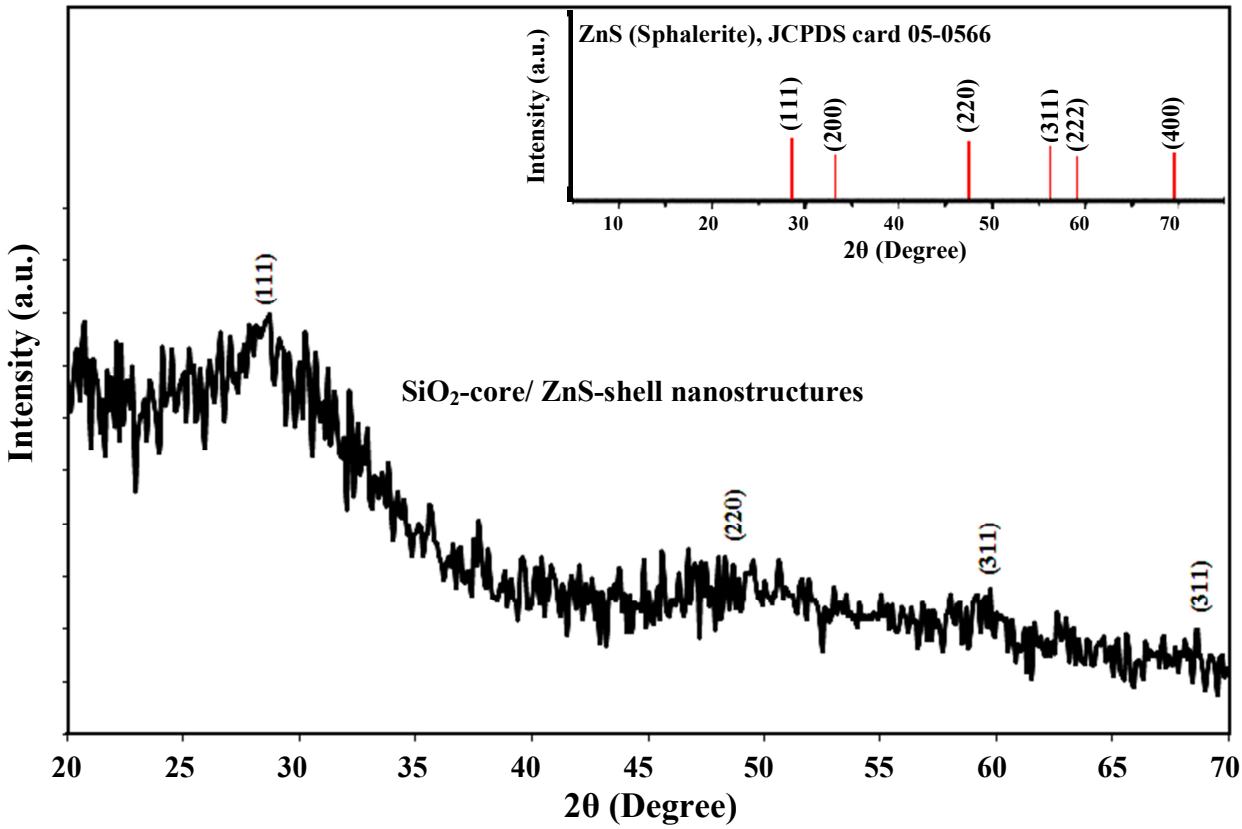

Fig. 2. XRD pattern of SiO_2/ZnS core-shell (inset: JCPDS card 05-0566).

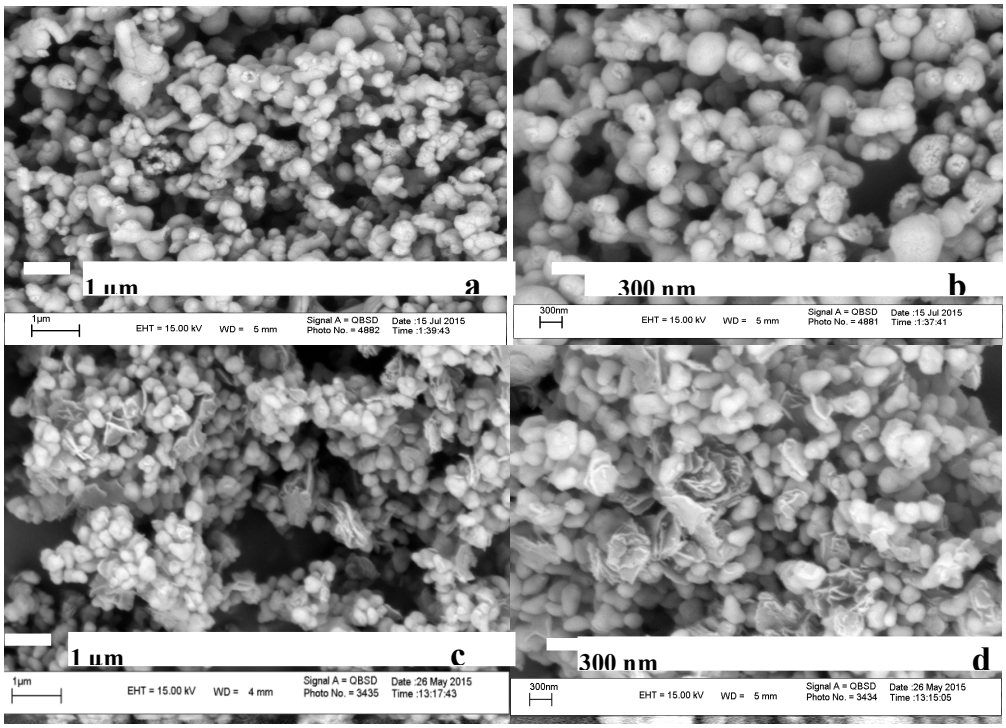

Fig. 3. Low and high magnifications SEM images for the pure SiO_2 particles (a and b), and SiO_2/ZnS nanostructures (c and d).

has been reduced, but the intensity of N–H bonding is slightly increased.

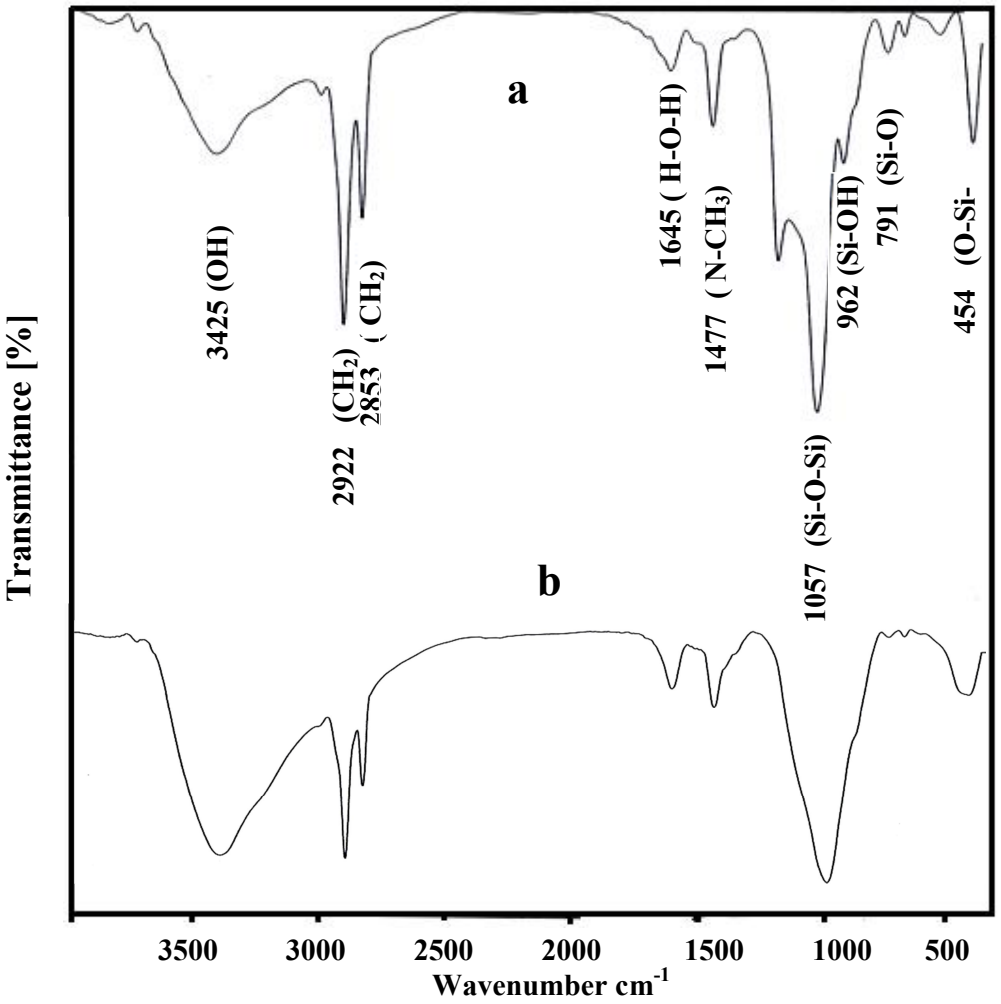

Fig. 4. FT-IR spectra of SiO_2 (a) and SiO_2/ZnS core-shell nanoparticle

The TEM analysis revealed the formation of the core-shell nanostructures (Fig. 5). We observed a grayish layer around the SiO_2 particles and the thickness of the layer was about only 14 nm which indicates the formation of a zinc sulphide shell on the particles surface.

The UV–vis diffused reflectance spectrum (UV–vis DRS) for Silica/ZnS nanoparticles is shown in Fig. 6. In common excitonic absorption and emission helps in understanding the purity of the samples and it gives information about the defects present in the crystal system. Comparing the absorption edge of bulk ZnS to that of SiO_2/ZnS core-shell, it is seen that a blue shift in the onset of absorption is observed in this sample. This blue shift indicates that ZnS exists as small clusters [13]. This phenomenon of blue shift of absorption edge has been ascribed to a decrease in particle size. It is well known that in case of semiconductors the band gap between the valence and conduction band increases as the size of the particle decreases in the nanosize range. This results in a shift in the absorption edge to a lower wavelength region. The magnitude of the shift depends on the

particle size of the semiconductor. The band gap of ZnS has been determined as 3.70 eV directly from the absorption maximum of ZnS, λ_{max} = 335 nm. The bandgap of the bulk ZnS is 3.54 eV. The band gap edge of CdS gets 0.16 eV blue shifted than bulk ZnS, which may be due to quantum confinement. The widened FWHM observed in XRD and morphological analysis also confirming the thinner ZnS shell layer.

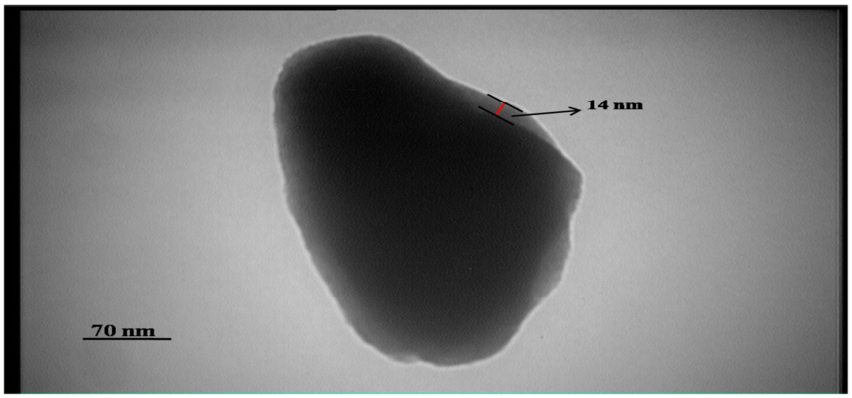

Fig. 5. Transmission electron microscopic image of SiO_2/ZnS core-shell nanostructure.

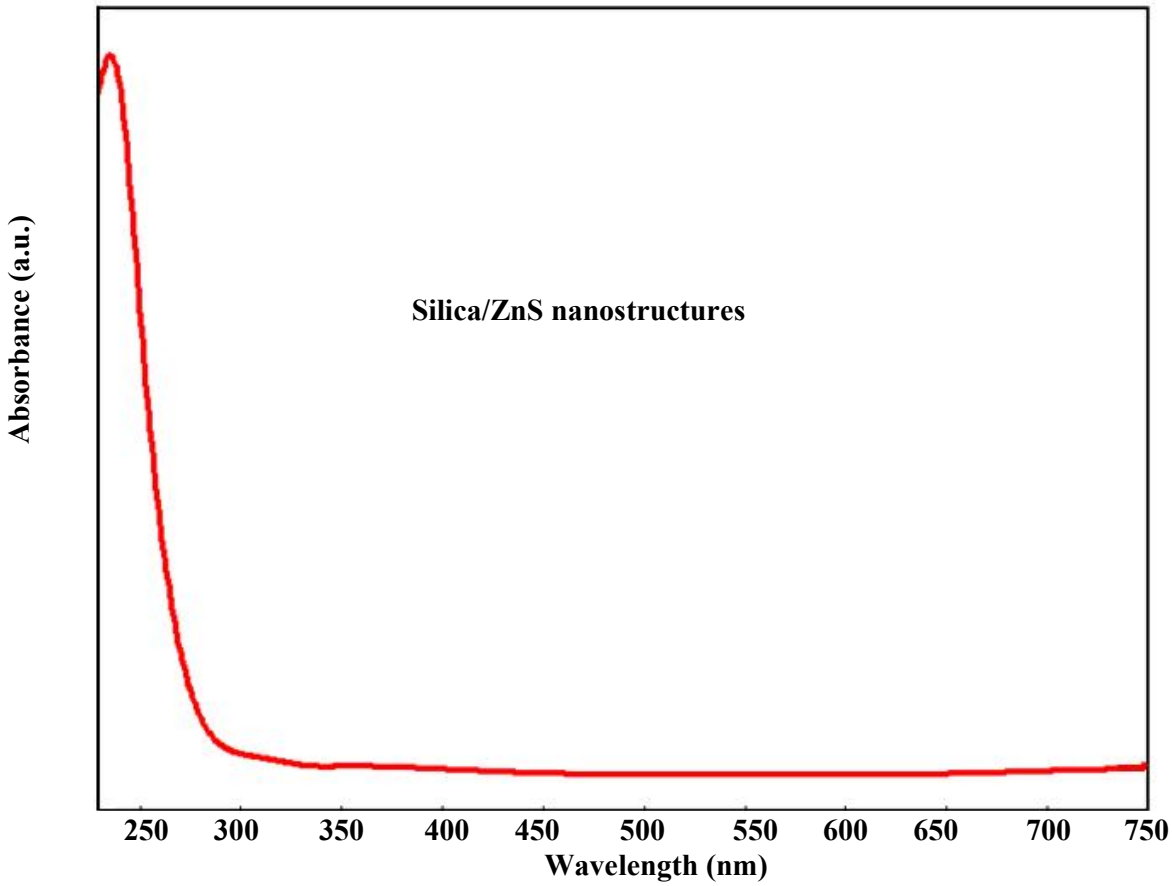

Fig. 6. UV–vis absorption spectrum of SiO_2/ZnS nanoparticle.

4. CONCLUSION

In summary, a simple room temperature wet chemical method was employed for the synthesis of ZnS nanoparticles, which has the virtues of simplicity, low cost, high yield and low environmental impact. XRD, TEM, BET and UV were used to characterize the phase composition, morphology, and optical property of the samples. The silica spheres of ~250 nm and the shell thickness of ~14 nm have been identified in the morphological studies. A large blue shift in the absorption edge was observed in the samples prepared by an ion-exchange method, indicating the formation of nanometer-sized ZnS nanoparticles, as a consequence of particle size effects.

ACKNOWLEDGEMENTS

Financial support by Rasht Branch, Islamic Azad University Grant No. 4.5830 is gratefully acknowledged.

REFERENCES

[1] Z. Yang, Y. Lu, Z. Yang, *Chem. Commun*. 0, 2270 (**2009**).
[2] A. Pourahmad, *Superlattice. Microst.* 52, 276 (**2012**).
[3] Y. Zhu, T. Mei, Y. Wang, Y. Qian, *J. Mater. Chem.* 21, 11457 (**2011**).
[4] J.-S. Hu, L.-L. Ren, Y.-G. Guo, H.-P. Liang, A.-M. Cao, L.-J. Wan, C.-L. Bai, *Angew. Chem. Int. Ed.* 44, 1269 (**2005**).
[5] M. D. Pre, I. Morrow, D. J. Martin, M. Mos, A. Del Negro, S. Padovani, A. Martucci, *Mater. Chem. Phys.* 139, 531 (**2013**).
[6] A. Le Donne, S. K. Jana, S. Banerjee, S. Basu, S. Binetti, *J. Appl. Phys.* 113, 014903 (**2013**).
[7] Z. N. Yu, J. Leng, W. Xue, T. Zhang, Y. R. Jiang, J. Zhang, D. P. Zhang, *Appl. Surf. Sci.* 258 2270 (**2012**).
[8] D. G. Chen, F. Huang, G. Q. Ren, D. S. Li, M. Zheng, Y. J. Wang, Z. Lin, *Nanoscale*. 2, 2062 (**2010**).
[9] Z. Y. Gao, N. Liu, D. P. Wu, W. G. Tao, F. Xu, K. Jiang, *Appl. Surf. Sci.* 258, 2473 (**2012**).
[10] R. I. Nooney, D. Thirunavukkarasu, Y. Chen, R. Josephs, A. E. Ostafin, *Chem. Mater.* 14, 4721 (**2002**).
[11] Y. Kievsky, I. Sokolov, *IEEE Trans. Nanotechnol.* 4, 490 (**2005**).
[12] W. Tang, F. Teng, Y. B. Hou, Y. S. Wang, F. R. Tan, S. C. Qu, Z. G. Wang, *Appl. Phys. Lett.* 96, 163112 (**2010**).
[13] A. Pourahmad, *Mater Lett.* 65, 2551 (**2011**).